

**Electrochemical CO₂ Reduction on Copper in Propylene Carbonate
Influence of Water Content and Temperature on the Product Distribution**

Burgers, Iris; Pérez-Gallent, Elena; Goetheer, Earl; Kortlever, Ruud

DOI

[10.1002/ente.202201465](https://doi.org/10.1002/ente.202201465)

Publication date

2023

Document Version

Final published version

Published in

Energy Technology

Citation (APA)

Burgers, I., Pérez-Gallent, E., Goetheer, E., & Kortlever, R. (2023). Electrochemical CO₂ Reduction on Copper in Propylene Carbonate: Influence of Water Content and Temperature on the Product Distribution. *Energy Technology*, 11(8), Article 2201465. <https://doi.org/10.1002/ente.202201465>

Important note

To cite this publication, please use the final published version (if applicable).
Please check the document version above.

Copyright

Other than for strictly personal use, it is not permitted to download, forward or distribute the text or part of it, without the consent of the author(s) and/or copyright holder(s), unless the work is under an open content license such as Creative Commons.

Takedown policy

Please contact us and provide details if you believe this document breaches copyrights.
We will remove access to the work immediately and investigate your claim.

Electrochemical CO₂ Reduction on Copper in Propylene Carbonate: Influence of Water Content and Temperature on the Product Distribution

Iris Burgers, Elena Pérez-Gallent, Earl Goetheer, and Ruud Kortlever*

Aqueous electrolytes are most commonly used for the CO₂ reduction reaction (CO₂RR), but suffer from a low CO₂ solubility that limits the reaction. Electrochemical CO₂ reduction in nonaqueous electrolytes can provide a solution, due to the higher CO₂ solubility of organic solvent-based electrolytes. Herein, the product distribution of the electrochemical CO₂ reduction on polycrystalline Cu in 0.7 M tetraethylammonium chloride in propylene carbonate with different water additions (0, 10, and 90 v%), and for different operating conditions (10, 25, 40, and 60 °C), is investigated. It is found that CO₂ reduction on Cu in a propylene carbonate solution results in H₂, CO, and formic acid formation only, even though Cu is known to produce C₂₊ products such as ethylene and ethanol in aqueous electrolytes. Increasing the operating temperature increases the CO₂RR kinetics and shows an improvement in CO formation and decrease in H₂ formation. However, increasing the operating temperature also increases water transport through the membrane, resulting in an increase of H₂ formation over time when operating at 60 °C.

1. Introduction

Currently most of our fuels and chemicals are produced from fossil feedstock, resulting in large amounts of CO₂ emissions from these processes which create a great threat on our environment. With decreasing renewable electricity prices and increasing availability of renewable electricity, the production of fuels and chemicals using electrochemistry becomes more interesting.^[1] In the electrochemical reduction of CO₂, electricity is used to convert CO₂ into value-added chemicals.^[2–4] With the

intermittent production of renewable electricity, the CO₂ reduction reaction (CO₂RR) can provide a means for long-term and large-scale storage of renewable energy in chemical bonds as well as a way to close the carbon cycle.^[5,6]


The choice of electrode material is key in electrochemical CO₂ reduction, as it determines which products are formed in the reduction reaction and the overall selectivity toward these products. Therefore, most studies on CO₂ reduction have focused on the design of selective and efficient catalysts and on obtaining insights in the possible reaction pathways for the different products.^[4,7–11] However, there are many more important factors that influence the CO₂RR, such as the electrolyte choice, including, for instance, cation and anion effects and operating conditions such as the local pH, pressure, and temperature.^[7,12–14]

Typically, aqueous electrolytes are used for CO₂RR. Unfortunately, the solubility of CO₂ in water is very low (≈34 mM).^[7,8,15] This significantly limits the amount of CO₂ present in the electrolyte and thereby limits the CO₂RR due to the limited mass transport of CO₂ to the electrode surface. Furthermore, the large amount of water present facilitates the hydrogen evolution reaction (HER), an undesired side reaction competing with CO₂ reduction in the same potential window.^[12]

One possible way to increase the CO₂ solubility and limit the HER is using organic solvents.^[7,12,16,17] There are a limited number of studies that investigate the reduction of CO₂ in organic solvents. Most studies have focused on electrolytes based on acetonitrile (ACN), methanol, propylene carbonate (PC), dimethyl sulfoxide (DMSO), and dimethylformamide (DMF).^[7,8,13] The main CO₂RR products observed in organic solvents are oxalic acid, CO, and carbonate (CO₃²⁻).^[7,8] Oxalic acid is formed through the dimerization of two free CO₂⁻ radicals in aprotic conditions. In the absence of water, CO and CO₃²⁻ are formed through a disproportionation reaction of a CO₂⁻ radical and CO₂. The formation of formic acid is only possible in the presence of water, by protonation of a CO₂⁻ radical and electron transfer.^[7,8] Although most organic solvents are capable of suppressing the HER, the current densities for CO₂ reduction are typically low, due to a lack of protons available for the reduction reaction. Therefore, several studies have suggested that CO₂ reduction in organic solvents can be significantly enhanced by adding small amounts of water, acting as a proton donor.^[18,19]

I. Burgers, E. Goetheer, R. Kortlever
Process and Energy
Delft University of Technology
2628 CB Delft, Zuid-Holland, The Netherlands
E-mail: R.Kortlever@tudelft.nl

E. Pérez-Gallent, E. Goetheer
Department of Sustainable Process and Energy Systems
TNO
2628 CA Delft, Zuid-Holland, The Netherlands

 The ORCID identification number(s) for the author(s) of this article can be found under <https://doi.org/10.1002/ente.202201465>.

© 2023 The Authors. Energy Technology published by Wiley-VCH GmbH. This is an open access article under the terms of the Creative Commons Attribution License, which permits use, distribution and reproduction in any medium, provided the original work is properly cited.

DOI: 10.1002/ente.202201465

Rudnev et al.^[18] demonstrated a strong promoting effect of water in ACN for the reduction of CO₂ on gold. Water is thought to serve as a proton donor, reducing the overpotential at which CO₂ reduction is taking place. However, this study only performed cyclic voltammetry (CV) experiments. Therefore, it is still unclear what effect water additions have on the product distribution of the CO₂RR. A previous study by Shi et al.^[19] studied the effect of adding 6.8 wt% water to PC for the reduction of CO₂ to CO on a gold cathode. PC was chosen as the preferred organic electrolyte as it has a large electrochemical operating window, high CO₂ solubility (134 mM), and is nontoxic.^[7,19] This study observed a decrease in the reduction potential during potentiostatic electrolysis, confirming that water acts as a catalyst for the CO₂RR toward CO. However, the authors did not measure the water concentration after electrolysis, nor did they investigate different water concentrations. Therefore, it is still unclear how and if the water concentration in the catholyte is influencing the product distribution. Furthermore, a recent study by Boor et al.^[20] investigated CO₂ reduction to oxalic acid on a lead electrode in a propylene carbonate electrolyte. The influence of the water content was investigated and the authors concluded that an increase in water concentration decreases the oxalic acid formation and increases byproduct formation (e.g., formate, glycolic acid, and glyoxylic acid). Currently, most studies investigating CO₂ reduction in organic solvents with water additions do not quantify the products formed during the reduction reaction. Therefore, there is a need for more studies reporting the product distribution of CO₂RR in organic solvents with the addition of small amounts of water.

Although most experimental studies are performed at ambient temperature and pressure, industrial electrochemical processes typically operate at elevated temperatures up to 80 °C.^[21] The main sources of heat generation are the applied overpotential and the resistive losses generated within the electrolyzer stack. Only a few studies have investigated the effect of temperature on the CO₂ reduction performance and product distribution.^[22–28] In general, increasing the temperature improves the ionic conductivity of the membrane and the electrocatalytic activity, but also enhances the membrane's chemical degradation processes and decreases CO₂ solubility.^[28,29] The earliest work on the effect of temperature on the CO₂RR dates back to 1986, by Hori and co-workers,^[22] who studied CO₂RR on a Cu electrode in a 0.5 M KHCO₃ solution at 5 mA cm⁻² in a temperature range from 0 to 40 °C. The amount of methane (CH₄) was found to decrease by increasing the temperature to 40 °C, whereas hydrogen (H₂), carbon monoxide (CO), and ethylene (C₂H₄) production increased. A similar trend was observed by Ahn et al.,^[26] using a polycrystalline copper electrode in a 0.1 M KHCO₃ solution at -1.60 V versus Ag/AgCl to study the reduction of CO₂ between 2 and 42 °C. A shift in selectivity from ethylene and formate to methane was observed when decreasing the temperature. The large amount of H₂ formation at higher temperatures is attributed to the decrease in dissolved CO₂. In addition, a recent systematic study performed by Vos et al.^[28] concluded that at elevated temperatures the increase in kinetics of CO₂RR is counteracted by the decrease in CO₂ solubility. The effect of temperature on CO₂RR so far has mainly been investigated in aqueous systems, with a limited amount of studies looking at the effect of temperature in non-aqueous electrolytes. Studies using nonaqueous electrolytes focus mainly on methanol or acetonitrile electrolytes at

temperatures around 243 K, based on the Rectisol method, to increase the methane formation.^[30–35] Additionally, Boor et al.^[20] studied CO₂ reduction to oxalic acid on a Pb electrode at 55 and 75 °C, using a PC electrolyte. They achieved the highest oxalic acid selectivities and current densities at 55 °C, due to the decrease in CO₂ solubility at higher temperatures. To the best of our knowledge, there are no studies that have investigated the effect of temperature on CO₂ reduction on a copper electrode using a nonaqueous electrolyte.

Here, we report on the product distribution of CO₂ reduction on a Cu electrode using 0.7 M TEACl in PC electrolyte. We investigate the effect of adding small amounts of water to the electrolyte and the effect of the operating temperature on the resulting product distribution.

2. Results and Discussion

2.1. Cyclic Voltammetry

To determine the potential window for CO₂ reduction on a Cu electrode in a 0.7 M TEACl in PC solution with varying concentrations of water (0, 10, and 90 v% water), CV experiments were performed in the presence and absence of CO₂. **Figure 1** shows the voltammograms with solid lines representing the argon (Ar)-saturated solutions, whereas the dotted lines represent the CO₂-saturated solutions. It is of importance to note that upon addition of water to the PC solvent, the CO₂ solubility will decrease. However, upon an addition of 10 v% of water, the CO₂ solubility is expected to only be slightly lower than for a pure PC electrolyte. Therefore, the decrease in dissolved CO₂ is expected to have a rather limited effect on the CO₂RR.

Figure 1 shows that in an Ar atmosphere a reductive current is observed with an onset potential of -2.1 V versus Ag/AgCl (solid green line) when there is no water added to the electrolyte. This suggests that at potentials of -2.1 V versus Ag/AgCl and lower,

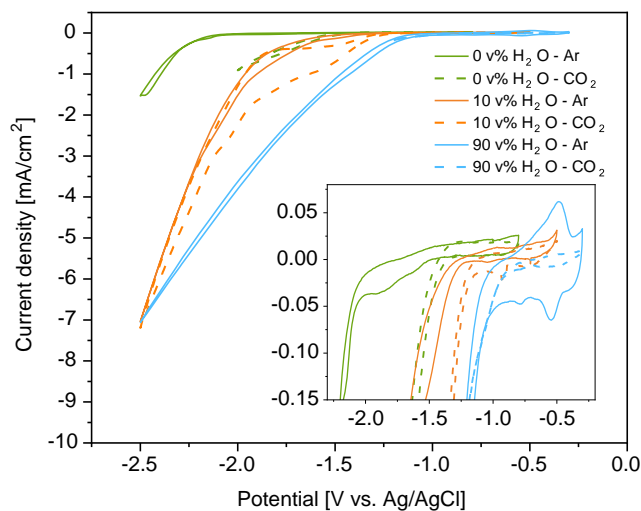


Figure 1. Cyclic voltammograms of a polycrystalline Cu electrode in a (–) argon saturated and (···) CO₂ saturated propylene carbonate with 0.7 M TEACl solution, with 0, 10, and 90 v% water addition, recorded at a scan rate of 20 mV s⁻¹. The insert displays a zoom-in between -0.25 V until -2.25 V vs. Ag/AgCl.

either PC or the supporting electrolyte salts (TEACl) decomposes. Upon adding 10 v% water to the electrolyte (solid orange line), the onset potential of the reductive current shifted to less negative potentials (-1.4 V vs. Ag/AgCl). Moreover, the slope of the reduction current increases at -2.0 V versus Ag/AgCl. We hypothesize that the first reductive current is related to H_2 formation, while the second reductive current is related to the reduction of the organic solvent. Increasing the water concentration further to 90 v% water (solid blue line) results in a further shift of the onset potential of the reductive current to -1.1 V versus Ag/AgCl. This current is assumed to be associated with H_2O reduction.

When the electrolyte with 0 v% water is saturated with CO_2 (dotted green line), there is a reductive current observed with an onset potential of -1.4 V versus Ag/AgCl that is associated with CO_2RR . When 10 v% water is added to the electrolyte (dotted orange line), a current associated with CO_2 reduction was observed with an onset potential of -1.2 V versus Ag/AgCl. The onset potential for the CO_2 -saturated electrolyte with 90 v% water (dotted blue line) is equal to the onset potential of the Ar-saturated solution (-1.1 V vs. Ag/AgCl) and no clear reduction current related to CO_2 reduction is observed.

From the voltammograms, a minimum and maximum cathode potential was selected to be applied in the chronoamperometry studies. A minimum potential of -1.6 V versus Ag/AgCl is chosen and the maximum applied potential is limited to -2.0 V versus Ag/AgCl to prevent decomposition of the electrolyte.

2.2. Chronoamperometry: The Effect of Water

Chronoamperometric (CA) studies for CO_2 reduction on Cu in a 0.7 M TEACl in PC electrolyte with 0, 10 and 90 v% water were performed for 1 h, with the aim of determining the product distribution of CO_2RR . The water concentration was limited to 10 v% due to solubility limit of water in PC, as with higher water concentrations the electrolyte behaves as a two-phase system. During these measurements, gaseous products were analyzed with an inline gas chromatograph, while liquid samples were taken from the electrolyte after the measurements to measure the liquid products formed.

Figure 2 shows the Faradaic efficiencies of all the products detected during CO_2RR on Cu with different concentrations of water added to the 0.7 M TEACl in PC solution at three different potentials: 1) -1.6 V versus Ag/AgCl, 2) -1.8 V versus Ag/AgCl, and 3) -2.0 V versus Ag/AgCl. All Faradaic efficiencies are averaged over the last 20 min of the experiment when the measured current was stable. For all three water concentrations, three main products were detected: hydrogen (H_2), carbon monoxide (CO), and formic acid (HCOOH). Besides these products, trace amounts of methane (CH_4) and ethylene (C_2H_4) were detected. The CO_2RR on Cu in a 0.7 M TEACl in PC electrolyte without added water does not form any methane or ethylene. Instead, formic acid is formed as major product next to H_2 . The formic acid concentration decreased with increasing the water concentration from 0 to 10 v%. When the water content in the catholyte increases from 10 to 90 v%, the system starts behaving more as an aqueous system and therefore the product selectivity is shifted toward H_2 and CO formation at all three applied potentials. However, ethylene is not detected and only small amounts of CH_4 are observed with an applied potential of -2.0 V versus Ag/AgCl (see Figure 2c). The catholyte with 90 v% water in PC was expected to perform similarly as an aqueous system. Even with 90 v% water present, no ethylene or other hydrocarbons are formed, which suggests that the presence of PC is somehow limiting the CO_2RR to hydrocarbons.

As expected, H_2 formation increases with increasing the water concentration for all three potentials. Even in the electrolyte with 0 v% water addition, a large amount of H_2 is formed. It is important to note that 0 v% water content refers to the freshly prepared electrolyte, where no water was added to it. However, during electrolysis, water from the aqueous anolyte diffuses through the membrane to the catholyte, due to the water concentration gradient and due to electro-osmotic drag.^[36] The effect of the electro-osmotic drag is increased as the applied potential increases. Moreover, the Nafion membrane is stored in water for activation and therefore can also slightly contribute to an increase in water concentration after electrolysis. The water content after electrolysis was measured with coulometric Karl–Fisher (KF) titration (see Figure S3, Supporting Information). After electrolysis, the water content of the electrolyte with 0 v% water addition increased from 0.2 v% to around 4 v%, whereas the water content

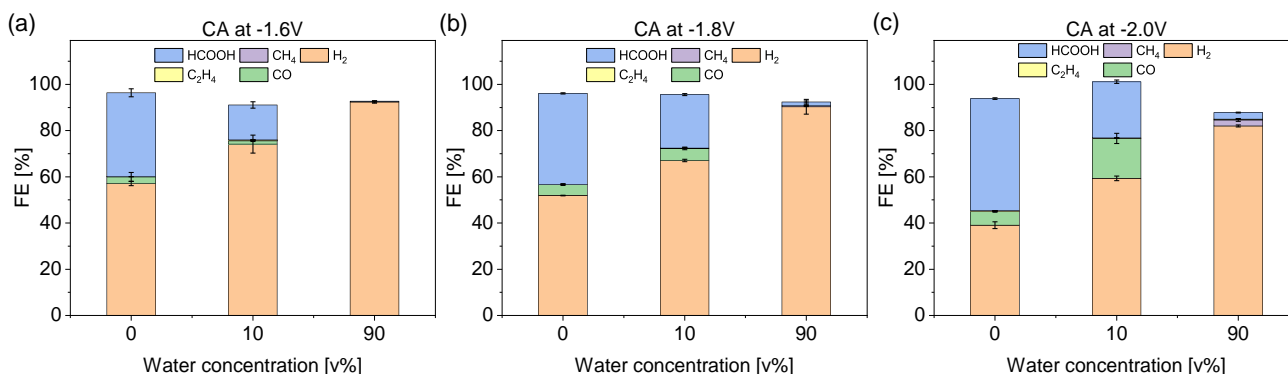


Figure 2. Chronoamperometry (CA) on a Cu electrode in 0.7 M TEACl in PC electrolyte at different potentials as a function of electrolyte water additions (0, 10, and 90 v% water). Faradaic efficiencies for a) CA at -1.6 V vs. Ag/AgCl, b) CA at -1.8 V vs. Ag/AgCl, and c) CA at -2.0 V vs. Ag/AgCl. Error bars indicate differences between duplicate measurements.

of the electrolytes with 10 and 90 v% water added remain the same. Nonetheless, for both electrolytes with 0 and 10 v% water addition, there is a decreasing trend in H₂ production when the applied potential is increased, whereas an increase in CO production is observed.

To eliminate the water present in the entire system, the anolyte was replaced with a nonaqueous solution, equal to the composition of the catholyte, and a chronoamperometry experiment was performed. In **Figure 3**, the CA results at -2.0 V versus Ag/AgCl are presented for a system with: 1) 0.7 M TEACl in PC with 0 v% water added as catholyte and anolyte (C: 0|A: 0), 2) 0.7 M TEACl in PC with 0 v% water added as catholyte and an aqueous anolyte (C: 0|A: 100), and 3) 0.7 M TEACl in PC with 10 v% water added and aqueous anolyte (C: 10|A: 100). The current obtained when using 0.7 M TEACl in PC as anolyte and catholyte (red line in Figure 3a) is lower in comparison to using an aqueous anolyte (green and purple line). The products detected for chronoamperometry measurements with a PC-based catholyte and anolyte are mainly formic acid, H₂, and CO, and small amounts of ethylene (Figure 3b) with formic acid as the main product formed. Furthermore, the amount of CO formed without water present in the catholyte and anolyte is similar to the amount of CO formed when using 10 v% water in a PC catholyte and an aqueous anolyte.

The total amount of water measured after 1 h of electrolysis is represented in Figure 3c. Without water additions to the anolyte or catholyte, the total amount of water measured in the catholyte is around 1.3 v% (Figure 3c C: 0|A: 0). The blank catholyte contains around 0.2 v% water, which means that there is still water entering the catholyte. The source of the water must be due to the use of a wet Nafion membrane, which needs to be activated in water. There is a direct relation between the amount of H₂ produced and the water concentration at the end of electrolysis: reducing the water concentration results in a reduced amount of H₂ produced. The suppression of the HER under the studied conditions did however not improve the CO₂RR selectivity toward hydrocarbon products, but only toward the CO and formic acid.

There are a limited amount of studies of CO₂ reduction in nonaqueous systems that use a Cu electrode.^[31,32,35] These studies used methanol as electrolyte and operated at temperatures below 273 K. Murugananthan et al.^[35] showed the best Faradaic

efficiency toward CH₄ of 37.5% at -4 V versus Ag quasi reference electrode at 243 K by increasing the pressure to 4 bar. In this work, the electrolysis is performed at different operating conditions and with PC instead of methanol, making it difficult to compare results and understand why in this study hydrocarbons were detected while here this is not the case. For Cu electrodes in aqueous systems, it is known that Faradaic efficiencies toward ethylene and ethanol in a 0.1 M KHCO₃ electrolyte range up to 30% and 10%, respectively, depending on the applied potential.^[37–39] We expect that the interaction of the solvent and the electrode in the double layer influences the binding strength of the different intermediates. **Figure 4** illustrates the different pathways in CO₂RR. The yellow path represents the formation of formate. In blue, the reaction pathway toward CO is presented. Due to the higher CO solubility in PC compared to water, it is expected that in PC electrolytes CO will desorb more readily from the surface.^[40,41] This results in a lower CO coverage on the copper electrode and thus prevents CO–CO dimerization and the further reduction of CO to hydrocarbons such as ethylene and ethanol (pathway in orange), which could explain why hydrocarbons are not formed in our system. Furthermore, if there is enough adsorbed hydrogen present on the surface, further reduction of CO to CH₄ is possible (pathway in green).^[8,42] However, due to the lack of water present in our system, the amount of adsorbed hydrogen on the surface is expected to be limited and this will in turn limit CH₄ formation. Finally, dimerization of the C₁ intermediates can also result in the formation of multicarbon products. This pathway will however also be limited due to the relatively lower coverage of hydrogen on the surface.

In aqueous systems, it is well known that alkali metal cations have a large impact on the selectivity and activity of the CO₂RR.^[3,15,43,44] Therefore, an initial chronoamperometry experiment was performed with 0.1 M KClO₄ in PC at -1.8 V (see Figure S5, Supporting Information). Due to solubility limitations of alkali metal salts in PC, it was not possible to perform a one-on-one comparison. More details can be found in the Supporting Information. The use of an alkali cation did not increase the amount hydrocarbon products and only resulted in the formation of H₂. This indicates that alkali metal cations do not affect the CO₂RR in nonaqueous systems the same way as in aqueous systems.

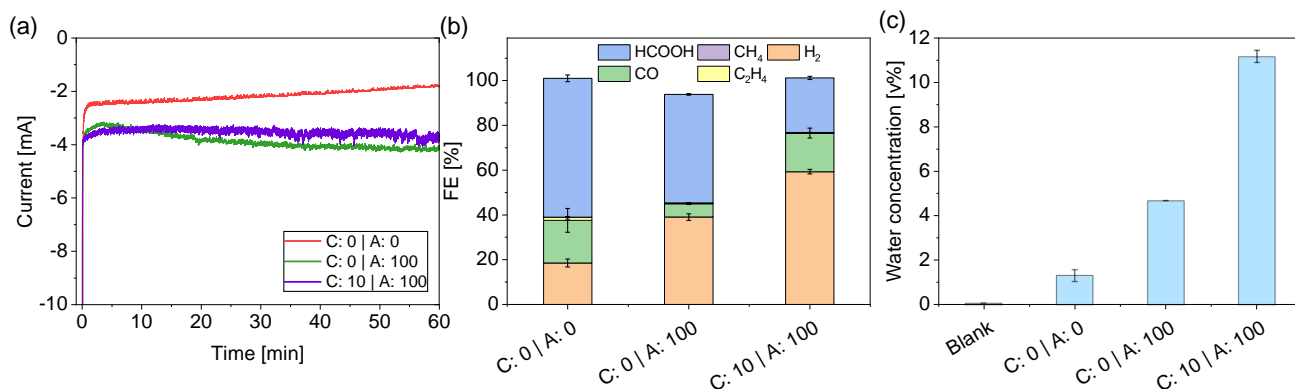


Figure 3. Chronoamperometry at -2.0 V vs. Ag/AgCl on a Cu electrode comparing i) 0.7 M TEACl in PC with 0% water added as catholyte and anolyte (C: 0|A: 0), ii) 0.7 M TEACl in PC with 0% water added as catholyte and an aqueous anolyte (0.5M H₂SO₄) (C: 0|A: 100), and iii) 0.7 M TEACl in PC with 10 v% water added and aqueous anolyte (C: 10|A: 100). a) Current density, b) faradaic efficiencies, and c) water concentrations before (blank) and after 1 h of CA for the three different electrolyte combinations. Error bars indicate differences between duplicate measurements.

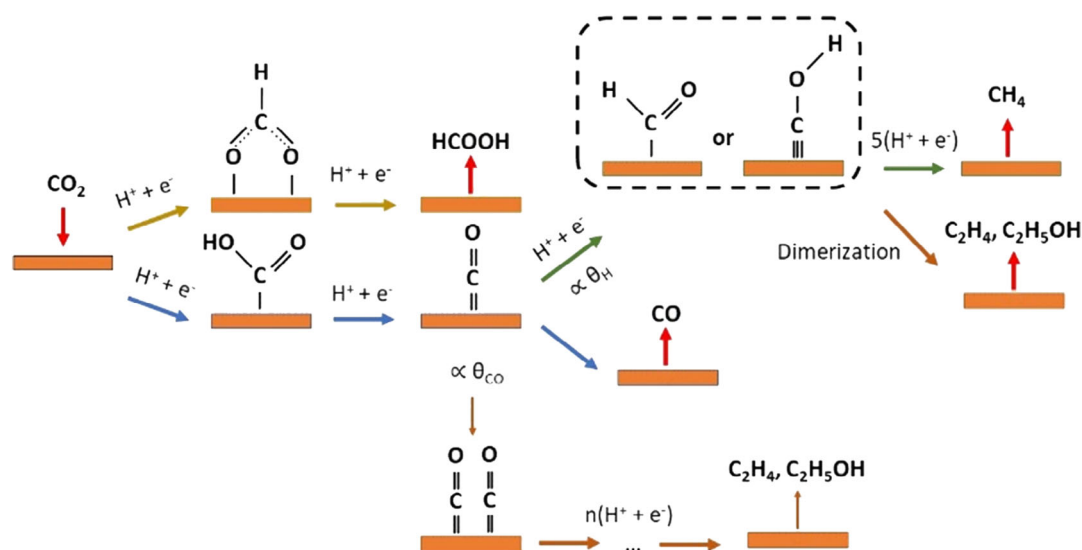


Figure 4. Schematic of different possible pathways for electrocatalytic CO₂ reduction. The yellow pathway leads to formate, blue pathway to CO, orange pathway toward multi-carbon products, and green path way to methane production.

One other possible way of increasing the selectivity toward ethylene is by increasing the operating temperature.^[22,26] Therefore, the next section will further explore the effect of operating temperature on the reduction of CO₂ on Cu in a 0.7 M TEACl/PC electrolyte.

2.3. Chronoamperometry: The Effect of Temperature

The effect of temperature during CO₂RR on Cu electrodes in PC-based electrolytes was studied using a slightly adapted flow-cell design (see Figure S1, Supporting Information). The cell was heated using a water bath and the temperature was kept constant throughout the electrolysis experiment. 1 h electrolysis experiments at -1.8 V versus Ag/AgCl were performed at 10, 25, 40, and 60 °C, using a 0.7 M TEACl in PC catholyte and aqueous anolyte (0.5 M H₂SO₄). The results are shown in **Figure 5**. The electrolysis results at 25 °C represent the same data as presented in Figure 2c for 0 v% water added to the organic electrolyte.

An increase of the electrolyte temperature results in a decrease in ohmic losses, as the conductivity of the electrolyte and membrane increases.^[25,28] This results in a higher current response at -1.8 V versus Ag/AgCl as the operating temperature increases, ranging from -2 mA cm⁻² at 10 °C to -6 mA cm⁻² at 60 °C (see Figure 5a).

Figure 5b shows that decreasing the temperature to 10 °C results in the formation of only H₂ and formic acid whereas at temperatures higher than 10 °C CO and traces of CH₄ and C₂H₄ were detected. Several studies concluded that decreasing the temperature also increases CH₄ formation in both aqueous and nonaqueous systems.^[26,30–35] However, at 10 °C in 0.7 M TEACl in PC, no CH₄ was detected as CO₂RR product on a Cu electrode. The previously mentioned studies using nonaqueous systems all used methanol-based electrolytes, which is a protic solvent. Since PC is aprotic, we anticipate that there are not enough protons present to form CH₄ and thus no increase in CH₄ formation at lower operating temperatures is observed in our system. The total Faradaic efficiency towards H₂ at 10 °C

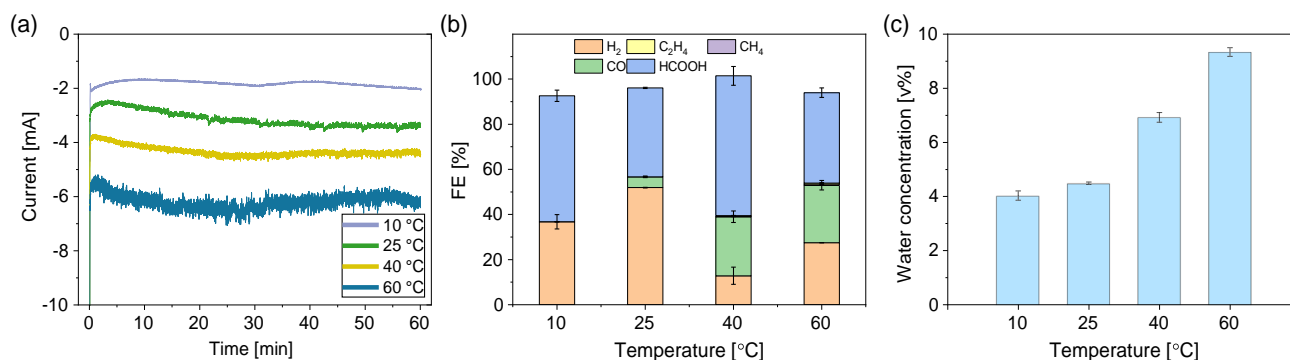


Figure 5. a) Current density, b) faradaic efficiency, and c) water concentration after 1 h of chronoamperometric measurements on Cu electrode in a 0.7 M TEACl in propylene carbonate solution containing 0 v% water at -1.8 V vs. Ag/AgCl at different temperatures. Error bars indicate differences between duplicate measurements.

slightly decreased to 37% as compared to 52% when operating at 25 °C. Previous studies confirm that the H₂ production decreases with decreasing operating temperatures.^[22–24,26] However, in our experiments the Faradaic efficiency toward H₂ also decreases at elevated temperatures, with a decrease to 13% at 40 °C and to 27% at 60 °C.

Interestingly, the Faradaic efficiency toward formic acid increased from 40% at 25 °C to 62% at 40 °C, but then decreased again to 40% at 60 °C. Furthermore, an increase in CO formation of 5% and 26% was observed when increasing the temperature from 25 to 40 °C and 60 °C respectively. Earlier studies on temperature effects showed that the increase in temperature resulted in an increase in reaction kinetics, but also in a decrease of CO₂ solubility.^[28] However, as described by Vos et al.,^[28] in aqueous systems, the increased reaction kinetics obtained when operating at higher operating conditions are not severely counteracted by the decrease in CO₂ solubility. Analogues to an aqueous system, this is expected to be similar in a PC electrolyte. The increased kinetics will lead to a higher formation rate of CO₂RR products, which is indeed observed in the partial current density toward CO for different operating temperatures (see Figure S7, Supporting Information). At 60 °C ethylene was detected, albeit in very small amounts (FE_{C₂H₄} = 0.76%). This suggests that the reaction kinetics can be improved toward ethylene when

increasing the temperature further, which is similar for aqueous systems.^[22] It is however not feasible to operate the Nafion membrane at higher temperatures, as the conductivity of the membrane significantly reduces above 80 °C.^[45]

The total amount of water measured after electrolysis for each operating temperature is presented in Figure 5c. The total amount of water measured increases with increasing operating temperature, as the permeability of the membrane increases at higher temperatures.^[29] Therefore, more water was transported through the membrane from the anolyte to the catholyte during the experiment, resulting in the highest water concentration of around 9 v% water when CO₂ electrolysis was conducted at 60 °C. This increase in water concentration in the catholyte at higher operating temperatures contributes to an increase in H₂ formation. All Faradaic efficiencies presented in Figure 5 are averaged over the last 20 min of the experiment when the measured current was stable. However, the product distribution over time, specifically at 60 °C, showed a clear trend where the H₂ concentration continuously increases and CO and C₂H₄ concentrations start to decrease (see Figure S6, Supporting Information). When running the CA for longer than 1 h at 60 °C, H₂ formation is expected to keep increasing as water will continue to be transported through the membrane. A similar trend was observed in terms of product distribution for experiments performed at

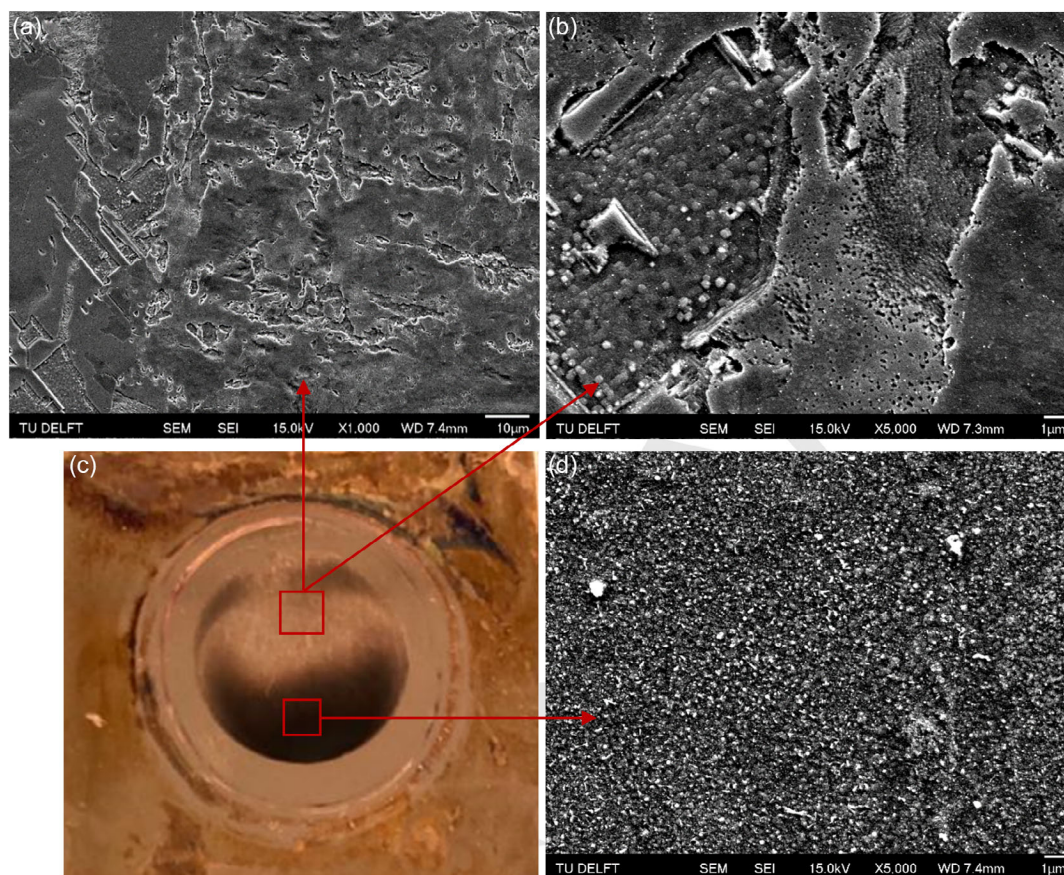


Figure 6. SEM images of the Cu electrode after chronoamperometry at -1.8 V for in a 0.7 M in propylene carbonate solution with 0 v% water additions, at 60 °C at a magnification of a) $1000\times$, b) $5000\times$, and d) $5000\times$. In (c) a picture of the electrode after electrolysis at 60 °C is shown, which clearly shows the change in surface colour.

40 °C. However, the trend was less pronounced as compared to the results of electrolysis at 60 °C.

2.4. Morphology Characterization

Scanning electron microscopy (SEM) was used to study the morphology changes of the copper foil before and after electrolysis at different operating temperatures. As expected, the surface undergoes structural transformations during electrolysis because of the reactions taking place.^[46] Figure 6a,b,d shows an increased surface roughening when operating the cell at 60 °C as compared to 25 °C (see Figure S7, Supporting Information). More and larger height differences were observed as well as more agglomeration and reshaping of the copper surface.

Furthermore, a black layer was observed on the copper surface after electrolysis at 60 °C (see Figure 6c). Energy-dispersive X-ray spectroscopy (EDS) results showed that in this black layer an increase in C atoms and O atoms occurred compared to the rest of the electrode surface. At the rest of the surface, the composition of the Cu electrode is equal to the composition of the Cu electrode after electrolysis at 25 °C (see Table S1, Supporting Information). Earlier work in aqueous solutions reported a similar poisoning process, where a thin black graphitic carbon layer was formed on the Cu electrode.^[23] In the blank tests with Ar instead of CO₂ under the same conditions, no products or black layer were detected, meaning that the used electrolyte was stable. This strongly indicates that the observed graphitic layer is formed as a consequence of intermediates of CO₂ decomposing on the electrode, similarly to aqueous systems. The graphitic carbon is expected to form via a side reaction, in which CO₂ is reduced through formate to graphitic carbon. It is therefore expected that the black layer has a significant role in the loss of the cathode performance in the CO₂ reduction at 60 °C, which was observed at the end of the 1 h electrolysis experiment (see Figure S6, Supporting Information).

3. Conclusion

Electrochemical CO₂ reduction on Cu electrodes in a 0.7 M TEACl in propylene carbonate catholyte has shown to produce mainly H₂, CO, and formic acid. It remains unclear what mechanism is preventing the reduction of CO₂ to hydrocarbon products on a Cu electrode when employing a PC electrolyte in comparison with CO₂RR in aqueous media. The influence on the product distribution during CO₂RR when increasing the water concentration in PC electrolyte was studied. Increasing the water content of the organic catholyte from 0 to 10 v% enhanced the formation of H₂ and CO while formic acid production decreased. Due to the aqueous nature of the anolyte used, water was transported through the membrane, and thus even when no additional water was added to the PC catholyte; around 4 v% water was measured in the catholyte after electrolysis which promoted H₂ production. By eliminating the aqueous anolyte and replacing it with a nonaqueous solvent, the HER can be suppressed further. As a result, an increase in formic acid and CO formation was observed. Furthermore, the effect of the operating temperatures on the CO₂RR in a PC-based electrolyte was studied and it was observed that increasing the operating temperature

increased the CO formation. However, due to the increased temperature, the amount of water transported through the membrane also increased. Particularly at 60 °C, this resulted in an increasing trend of H₂ formation and a decreasing trend in CO and C₂H₄ formation. Finally, SEM images showed that the stability of the Cu electrode was reduced at higher operating temperatures, as shown by surface roughening which occurred after electrolysis at 60 °C as compared to electrolysis at 25 °C.

4. Experimental Section

Electrode Surface Area Preparation: Copper foil (Aldrich 99.999%, 1 mm thickness, 2.5 cm × 2.5 cm) was used as working electrode. Initial sanding (up to grain size 2000) and polishing (up to 1 μm grade diamond paste) of the copper electrode were done to make sure no visible scratches were present on the copper. Prior to each experiment, electropolishing of the copper in phosphoric acid (85% in H₂O, Aldrich) at 2.1 V versus a graphite rod as counter electrode was performed for 3 min, based on Kuhl et al. SEM and EDS were used to characterize the electrode surface before and after electrolysis.

Electrochemical Cell: All experiments were performed in a two-compartment batch electrolyzer, based on the design of Lobaccaro et al.^[47] CO₂ was continuously bubbled at 8 mL min⁻¹ through the catholyte during the chronoamperometry experiments. The anolyte used was a 0.5 M aqueous H₂SO₄ (except otherwise stated) and the catholyte 0.7 M tetraethylammonium chloride (TEACl) in propylene carbonate (PC) with different concentrations of water (0, 10 and 90 v%). To prevent any contamination, the cell was stored in 20% v/v nitric acid and rinsed with MilliQ water before use.

Furthermore, a platinum counter electrode (MaTeck 99.99%, 0.1 mm thickness, 2.5 cm × 2.5 cm) and a leak-free Ag/AgCl reference electrode (Innovative Instruments LF-1-45) were used. A cation exchange membrane (Nafion-117) separated the anolyte and catholyte compartments. A potentiostat (SP-200, BioLogic) was used to perform the CV and chronoamperometry experiments.

The two-compartment electrochemical cell was modified for the high-temperature experiments (see Figure S1, Supporting Information). The back plates were replaced with aluminum back plates, which were heated using a water bath. The heated back plates were indirectly in contact with the electrodes and thus heating the electrolyte. An electrically insulating rubber gasket was placed in between the aluminum back plates and the electrodes, to prevent electricity passing through. The temperature of the anolyte was continuously measured during the experiment and kept constant. The thermocouple interfered with the measured current signal by the reference electrode; therefore it was not possible to measure the catholyte temperature during electrolysis. However, the anolyte and catholyte temperatures can be presumed to be equal. The chronoamperometry experiment was started as the soon as the anolyte was at the desired temperature.

Gas and Liquid Product Analysis: The compact H-cell was coupled to a gas chromatograph (Compact GC 4.0, Interscience) equipped with two thermal conductivity detectors and one flame ionization detector that measured the gaseous products formed in the cathode compartment with 2 min intervals during experiments. At the end of the experiment, samples of the electrolytes were analyzed using a high-pressure liquid chromatograph (HPLC) (1290 Infinity II, Agilent). For HPLC analysis, 5 μl of the catholyte solution was injected on two Aminex HPX-87H columns (Biorad) placed in series. The columns were heated to 60 °C, using an eluent containing 1 mM H₂SO₄ in ultrapure water and a refractive index detector (RID) for the detection of products. Coulometric KF (Metrohm 756 KF Coulometer) was used for the water content measurement before and after the experiment.

Supporting Information

Supporting Information is available from the Wiley Online Library or from the author.

Acknowledgements

This project received funding from the NWO-AES Crossover programme under project number 17621 (RELEASE).

Conflict of Interest

The authors declare no conflict of interest.

Data Availability Statement

The data that support the findings of this study are available from the corresponding author upon reasonable request.

Keywords

electrocatalysis, electrochemical CO₂ reduction, organic solvents, temperature effects, water effects

Received: February 1, 2023

Revised: March 29, 2023

Published online: May 5, 2023

- [1] R. Xia, S. Overa, F. Jiao, *J. Am. Chem. Soc. Au* **2022**, 2, 1054.
- [2] D. M. Weekes, D. A. Salvatore, A. Reyes, A. Huang, C. P. Berlinguette, *Acc. Chem. Res.* **2018**, 51, 910.
- [3] Y. Y. Birdja, E. Pérez-Gallent, M. C. Figueiredo, A. J. Göttle, F. Calle-Vallejo, M. T. M. Koper, *Nature Energy* **2019**, 4, 732.
- [4] O. Gutiérrez-Sánchez, Y. Y. Birdja, M. Bulut, J. Vaes, T. Breugelmans, D. Pant, *Curr. Opin. Green Sustainable Chem.* **2019**, 16, 47.
- [5] A. Chandrasekar, D. Flynn, E. Syron, *Int. J. Hydrogen Energy* **2021**, 46, 28900.
- [6] O. S. Bushuyev, P. De Luna, C. T. Dinh, L. Tao, G. Saur, J. van de Lagemaat, S. O. Kelley, E. H. Sargent, *Joule* **2018**, 2, 825.
- [7] M. König, J. Vaes, E. Klemm, D. Pant, *iScience* **2019**, 19, 135.
- [8] R. Kortlever, J. Shen, K. J. Schouten, F. Calle-Vallejo, M. T. Koper, *J. Phys. Chem. Lett.* **2015**, 6, 4073.
- [9] Q. Lu, F. Jiao, *Nano Energy* **2016**, 29, 439.
- [10] W. Zhang, Y. Hu, L. Ma, G. Zhu, Y. Wang, X. Xue, R. Chen, S. Yang, Z. Jin, *Adv. Sci.* **2018**, 5, 1700275.
- [11] S. Liang, N. Altaf, L. Huang, Y. Gao, Q. Wang, *J. CO₂ Util.* **2020**, 35, 90.
- [12] M. Moura de Salles Pupo, R. Kortlever, *ChemPhysChem* **2019**, 20, 2926.
- [13] S. Garg, M. Li, A. Z. Weber, L. Ge, L. Li, V. Rudolph, G. Wang, T. E. Rufford, *J. Mater. Chem. A* **2020**, 8, 1511.
- [14] H. Jhong, S. Ma, P. J. A. Kenis, *Curr. Opin. Chem. Eng.* **2013**, 2, 191.
- [15] S. Nitopi, E. Bertheussen, S. B. Scott, X. Liu, A. K. Engstfeld, S. Horch, B. Seger, I. E. L. Stephens, K. Chan, C. Hahn, J. K. Norskov, T. F. Jaramillo, I. Chorkendorff, *Chem. Rev.* **2019**, 119, 7610.
- [16] E. Sargeant, P. Rodríguez, *Electrochem. Sci. Adv.* **2022**.
- [17] A. R. Woldu, Z. Huang, P. Zhao, L. Hu, D. Astruc, *Coord. Chem. Rev.* **2022**, 454, 214340.
- [18] A. V. Rudnev, U. E. Zhumaev, A. Kuzume, S. Vesztergom, J. Furrer, P. Broekmann, T. Wandlowski, *Electrochim. Acta* **2016**, 189, 38.
- [19] J. Shi, F. Shen, F. Shi, N. Song, Y. Jia, Y. Hu, Q. Li, J. Liu, T. Chen, Y. Dai, *Electrochim. Acta* **2017**, 240, 114.
- [20] V. Boor, J. Frijns, E. Perez-Gallent, E. Giling, A. T. Laitinen, E. L. V. Goetheer, L. J. P. van den Broeke, R. Kortlever, W. de Jong, O. A. Moulton, T. J. H. Vlught, M. Ramdin, *Ind. Eng. Chem. Res.* **2022**, 61, 14837.
- [21] F. M. Sapountzi, J. M. Gracia, C. J. Weststrate, H. O. A. Fredriksson, J. W. Niemantsverdriet, *Prog. Energy Combust. Sci.* **2017**, 58, 1.
- [22] Y. Hori, K. Kikuchi, A. Murata, S. Suzuki, *Chem. Lett.* **1986**, 15, 897.
- [23] D. W. DeWulf, T. Jin, A. J. Bard, *J. Electrochem. Soc.* **1989**, 136, 1686.
- [24] M. Azuma, K. Hashimoto, M. Hiramoto, M. Watanabe, T. Sakata, *J. Electrochem. Soc.* **1990**, 137, 1772.
- [25] E. J. Dufek, T. E. Lister, M. E. McIlwain, *J. Appl. Electrochem.* **2011**, 41, 623.
- [26] S. T. Ahn, I. Abu-Baker, G. T. R. Palmore, *Catal. Today* **2017**, 288, 24.
- [27] Z. Zhang, E. W. Lees, F. Habibzadeh, D. A. Salvatore, S. Ren, G. L. Simpson, D. G. Wheeler, A. Liu, C. P. Berlinguette, *Energy Environ. Sci.* **2022**, 15, 705.
- [28] R. E. Vos, M. T. M. Koper, *ChemElectroChem* **2022**, 9, e202200239.
- [29] F. Scheepers, M. Stähler, A. Stähler, E. Rauls, M. Müller, M. Carmo, W. Lehnert, *Appl. Energy* **2021**, 283, 116270.
- [30] S. Kaneco, K. Iiba, S. Suzuki, K. Ohta, T. Mizuno, *J. Phys. Chem. B* **1999**, 103, 7456.
- [31] S. Ohya, S. Kaneco, H. Katsumata, T. Suzuki, K. Ohta, *Catal. Today* **2009**, 148, 329.
- [32] A. Naitoh, K. Ohta, T. Mizuno, H. Yoshida, M. Sakai, H. Noda, *Electrochim. Acta* **1993**, 38, 2177.
- [33] S. Kaneco, K. Iiba, H. Katsumata, T. Suzuki, K. Ohta, *J. Solid State Electrochem.* **2006**, 11, 490.
- [34] Y. Oh, H. Vrubel, S. Guidoux, X. Hu, *Chem. Commun.* **2014**, 50, 3878.
- [35] M. Murugananthan, M. Kumaravel, H. Katsumata, T. Suzuki, S. Kaneco, *Int. J. Hydrogen Energy* **2015**, 40, 6740.
- [36] M. J. Cheah, I. G. Kevrekidis, J. Benziger, *J. Phys. Chem. B* **2011**, 115, 10239.
- [37] K. P. Kuhl, E. R. Cave, D. N. Abram, T. F. Jaramillo, *Energy Environ. Sci.* **2012**, 5, 7050.
- [38] Y. Hori, A. Murata, R. Takahashi, *J. Chem. Soc.* **1989**, 85, 2309.
- [39] S. Asperti, R. Hendriks, Y. Gonzalez-Garcia, R. Kortlever, *ChemCatChem* **2022**, 14, e202200540.
- [40] M. S. Shaharun, H. Mukhtar, B. K. Dutta, *Chem. Eng. Sci.* **2008**, 63, 3024.
- [41] U. J. Jáuregui-Haza, E. J. Pardillo-Fontdevila, A. M. Wilhelm, H. Delmas, *Lat. Am. Appl. Res.* **2004**, 34, 71.
- [42] A. R. T. Morrison, M. Ramdin, L. J. P. van der Broeke, W. de Jong, T. J. H. Vlught, R. Kortlever, *J. Phys. Chem. C* **2022**, 126, 11927.
- [43] A. Murata, Y. Hori, *Chem. Soc. Jpn.* **1991**, 64, 123.
- [44] E. Perez-Gallent, G. Marcandalli, M. C. Figueiredo, F. Calle-Vallejo, M. T. M. Koper, *J. Am. Chem. Soc.* **2017**, 139, 16412.
- [45] S. G. Avramov, E. Lefterova, H. Penchev, V. Sinigersky, E. Slavcheva, *Bulg. Chem. Commun.* **2016**, 48, 43.
- [46] S. Popovic, M. Smiljanic, P. Jovanovic, J. Vavra, R. Buonsanti, N. Hodnik, *Angew. Chem.* **2020**, 59, 14736.
- [47] P. Lobaccaro, M. R. Singh, E. L. Clark, Y. Kwon, A. T. Bell, J. W. Ager, *Phys. Chem. Chem. Phys.* **2016**, 18, 26777.